American Mineralogist, Volume 71, pages 686–693, 1986

Experimental study of subsolidus phase relations and mixing properties of clinopyroxene in the silica-saturated system CaO-MgO-Al_2O_3-SiO_2

TIBOR GASPARIK
Department of Earth and Space Sciences, State University of New York, Stony Brook, New York 11794

ABSTRACT

In the system CaO-MgO-Al_2O_3-SiO_2 (CMAS), the equilibrium compositions of the clinopyroxene coexisting with anorthite and quartz were experimentally determined at 20 different P-T conditions (1200–1400°C, 14.0–30.4 kbar), and those of the clinopyroxene coexisting only with anorthite were determined in 15 experiments, using PbO as flux. The data were fitted to the Redlich-Kister equation for a ternary solution, providing the following mixing properties of the $CaMgSi_2O_6$-$CaAl_2SiO_6$-$Ca_{0.5}AlSi_2O_6$ (Di-CaTs-CaEs) pyroxene (units: joules, kelvins, bars):

$$G_{Px}^{excess} = X_{CaTs}X_{Di}[10\,000 - 10T - 0.07P - (50\,000 - 31.19T + 0.04P)(X_{CaTs} - X_{Di}) - 7000(X_{CaTs} - X_{Di})^2] + X_{CaTs}X_{CaEs}[-20\,160 + 14\,760(X_{CaTs} - X_{CaEs})] + X_{Di}X_{CaEs}[-5950].$$

This solution model is consistent with the properties of the Di-CaTs binary determined previously, but does not give the correct CaTs-CaEs properties because of inferred anomalous mixing behavior of the ternary pyroxenes with low Di content.

The assemblages pyroxene + anorthite + quartz at lower pressures and pyroxene + garnet + kyanite + quartz at higher pressures are potentially useful as thermobarometers, applicable to quartz-bearing granulites and grospydites with low MgO and Na_2O contents.

INTRODUCTION

Clinopyroxenes in the system CaO-MgO-Al_2O_3-SiO_2 can have up to four components in solution: diopside (Di—$CaMgSi_2O_6$), Ca-Tschermak pyroxene (CaTs—$CaAl_2SiO_6$), Ca-Eskola pyroxene (CaEs—$Ca_{0.5}AlSi_2O_6$), and enstatite (En—$Mg_2Si_2O_6$). Diopside and Ca-Tschermak pyroxene are the only endmembers that are stable and can form a complete solid solution. The present study focuses on the silica-saturated CMAS system in which the clinopyroxene in equilibrium with anorthite (An), kyanite (Ky), or a silica polymorph incorporates variable amounts of the Ca-Eskola component. The En component, significant in the clinopyroxene coexisting with orthopyroxene and other MgO-rich phases, turned out to be negligible in the equilibria considered here.

Before the extent of solubility of the CaEs component in clinopyroxene was known, the silica-saturated CMAS system had appeared to provide an ideal opportunity for an experimental determination of mixing properties of the Di-CaTs solid solution. Such a study was carried out by Wood (1979), who investigated equilibria in the assemblage pyroxene (Px) + anorthite + quartz (Q). The major conclusion of Wood's study was that at 1 bar and 1200–1300°C, the activity of the CaTs component in solution with diopside approximately corresponded to its mole fraction. However, the pyroxene in equilibrium with anorthite and quartz contains, especially at higher pressures, significant amounts of the CaEs component (Wood and Henderson, 1978). Thus, the activities of the CaTs component determined by Wood (1979) do not apply to a pure Di-CaTs solution; instead, they are modified by the CaEs component. In the present study, which uses the same experimental approach as Wood (1979), the ternary-pyroxene properties were extrapolated to the Di-CaTs binary using a ternary-solution model. New experimental data were obtained for the following reasons:

1. The small size of pyroxene crystals in Wood's experimental products prevented the use of an electron microprobe, which can provide analyses of higher quality than the electron microscope microanalyzer used by Wood. In the present study, microprobe analyses were made possible by seeding starting materials with large pyroxene crystals.

2. Most of Wood's experiments were conducted at and below 20 kbar. Under these pressures, the pyroxene composition is quite insensitive to changes in P-T conditions, and only a limited range of the Di-rich compositions can be covered in experiments. In the present study, most of the experiments were conducted at higher pressures to cover a wider range of pyroxene compositions.

Preliminary results of this study were reported by Gasparik and Lindsley (1980) and Gasparik (1981). Since

0003–004X/86/0506–0686$02.00

then, the mixing properties of the Di-CaTs solution were determined by Gasparik (1984a) using equilibria in the assemblage pyroxene + garnet (Ga) + corundum (Cor). The latter approach avoided ambiguities caused by a model-dependent extrapolation of the ternary-pyroxene properties to the Di-CaTs binary, because the pyroxene in equilibrium with garnet and corundum contains, in addition to Di and CaTs, only minor amounts of the En component. The disadvantages of the latter approach are that the Di-rich pyroxene compositions cannot coexist with garnet and corundum and that the garnet is also a solid solution. Because neither of the two approaches for determining the properties of the Di-CaTs solution is perfect, the data from both studies were used to derive a set of mixing parameters for the Di-CaTs solution that satisfied all experimental observations.

Experimental techniques

General procedures

Experiments were carried out using a conventional piston-cylinder apparatus with a 0.5-in.-diameter assembly made of talc and boron nitride. Samples were encased in platinum capsules. The description of the assembly, its pressure calibration, and experimental procedures are in Gasparik (1985). For this assembly, the temperature-dependent pressure correction is $-(19 - 0.01T)$ percent, when T is in degrees Celsius.

The nominal pressures were maintained within ±200 bars of the desired value. Temperature was measured by W-3 Re vs. W-25 Re thermocouples and controlled automatically. No correction for the effect of pressure on emf was applied. Uncertainty in the temperature is less than ±5°C.

Starting materials

Starting materials were mechanical mixes made of ultrapure oxides, $CaSiO_3$, and $CaAl_2O_4$ (Table 1). PbO was used in the starting materials as flux to promote equilibration of charges. Large crystals (20–50 μm) of synthetic diopside and Ca-Tschermak pyroxene were added to the starting materials in the amounts of approximately 3 wt% each. The crystals reacted with the coexisting phases, approaching an equilibrium pyroxene composition from two different directions. Thus, the equilibrium compositions were reversed with respect to Di and CaTs, but not CaEs.

The original seed crystals change their composition by two processes: reconstruction and equilibration. In the first process, a new pyroxene of a presumably equilibrium composition nucleates on the surface of the original seed and replaces it by growing from the surface to the center of the crystal. At the same time, the center of the original seed changes its composition by equilibration. The process of reconstruction is more efficient than equilibration when the change of composition requires a coupled substitution. In such a case, the new pyroxene forms an irregular rim around the original seed, with the core having a composition that is much closer to the original composition than the rim, or unchanged at all. However, if the original seed composition is very different from the equilibrium composition, the equilibration process is much more efficient, and the result is a crystal with gradual zonation. It must be stressed that the rims do not form by synthesis from oxides used in the starting materials. The oxides fully react in the press by the time the initial pressure and temperature are reached. If quenched immediately, the experimental product is crystalline, with all phases already present. The crystalline matrix is very fine and unsuitable for microprobe analysis. Any rims around the seed crystals formed by synthesis from oxides are equally too fine to be detected by an electron microprobe.

Table 1. Compositions of starting materials (in moles)

Mix	$CaAl_2O_4$	$CaSiO_3$	MgO	SiO_2	PbO
A	0.60	0.40	0.40	2.60	0.25
B	0.50	0.50	0.50	2.50	0.20
C	0.60	0.40	0.40	2.60	0.40
D	0.70	0.30	0.30	2.50	0.25
E	0.70	0.30	0.30	2.50	0.40
F	0.70	0.30	0.30	2.50	0.10
G	0.80	0.20	0.20	2.60	0.40
H	0.80	0.20	0.20	2.60	0.30
I	0.80	0.20	0.20	2.60	0.20
J	0.85	0.15	0.15	3.45	0.30
K	0.85	0.15	0.15	3.45	0.20
L	0.85	0.15	0.15	2.55	0.05
M	0.90	0.10	0.10	2.50	0.10
N	0.90	0.10	0.10	2.50	0.05
O	0.93	0.07	0.07	2.43	0.15
P	0.70	0.30	0.30	1.90	0.25
Q	0.70	0.30	0.30	1.80	0.30
R	0.80	0.20	0.20	1.80	0.30
S	0.80	0.20	0.20	1.70	0.35
T	0.90	0.10	0.10	1.60	0.40
U	0.95	0.05	0.05	1.55	0.40
V	0.95	0.05	0.05	1.75	0.40
W	0.95	0.05	0.05	1.85	0.20
X	0.95	0.05	0.05	1.85	0.10
Y	1.00	-	-	1.60	0.20
Z	1.00	-	-	1.60	0.10
$	1.00	-	-	1.80	0.05

Analytical procedures

Experiments produced hard pellets composed of crystals surrounded by a PbO-rich glass. Approximately one half of a pellet was ground and used for phase identification by X-ray diffraction. The other half of the charge was mounted for microprobe analysis.

Wavelength-dispersive analyses were obtained with an automated ARL-EMX electron microprobe. All analyses were taken at 15-kV accelerating potential and 0.015-μA sample current on brass, using the minimum spot size (~1 μm). Standards were natural diopside for Ca, Mg, and Si, and natural anorthite for Al. The data were reduced using the correction procedures of Bence and Albee (1968). Analyses were obtained from the reaction rims developed around the seed crystals. The original compositions were preserved in the cores of the seeds; thus, it was always possible to infer the direction of the approach to equilibrium. Typically, 20–50 analyses were taken from several grains of each kind of seed. Only those pyroxene analyses were accepted that gave the sum of cations in the M1 and the T sites in the range 2.99–3.01. The concentrations of PbO in all crystalline phases were below the detection limit.

Experimental results

Equilibrium compositions of the clinopyroxene coexisting with anorthite and quartz were obtained at 20 different P-T conditions, and those of the clinopyroxene coexisting only with anorthite were determined in 15 experiments. For each experiment, average compositions of equilibrated rims on each kind of seed were calculated separately. The resulting averages obtained from the diopside and the CaTs seeds were then averaged to calculate the compositions used in the least-squares solution mod-

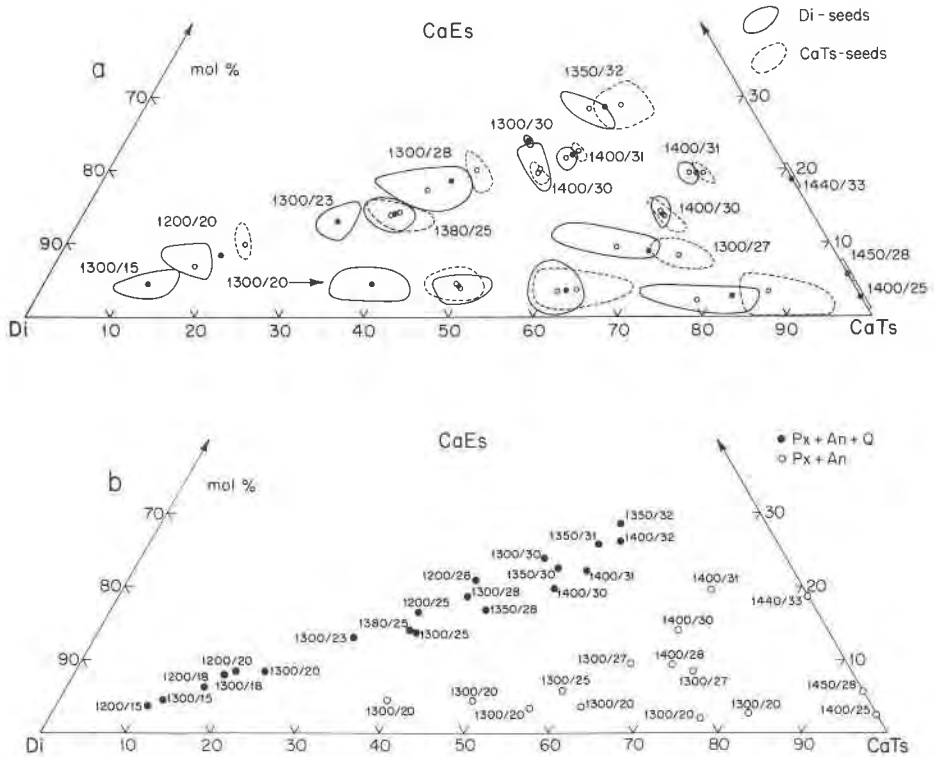

Fig. 1. Results of equilibration experiments containing the assemblages Px + An + Q and Px + An, shown in the compositional plane Di-CaTs-CaEs. Labeled: temperature (°C)/nominal pressure (kbar). (a) Pyroxene compositions from selected experiments. Shown are the typical compositional ranges observed in single experiments, and the variable degree of the approach to equilibrium. Envelopes enclose all accepted microprobe analyses. Average compositions calculated for each kind of seed (open circles) were averaged to produce the compositions used in the modeling (solid dots). (b) A complete set of the determined compositions of the pyroxene in equilibrium with anorthite and quartz (solid dots) and with anorthite only (open circles).

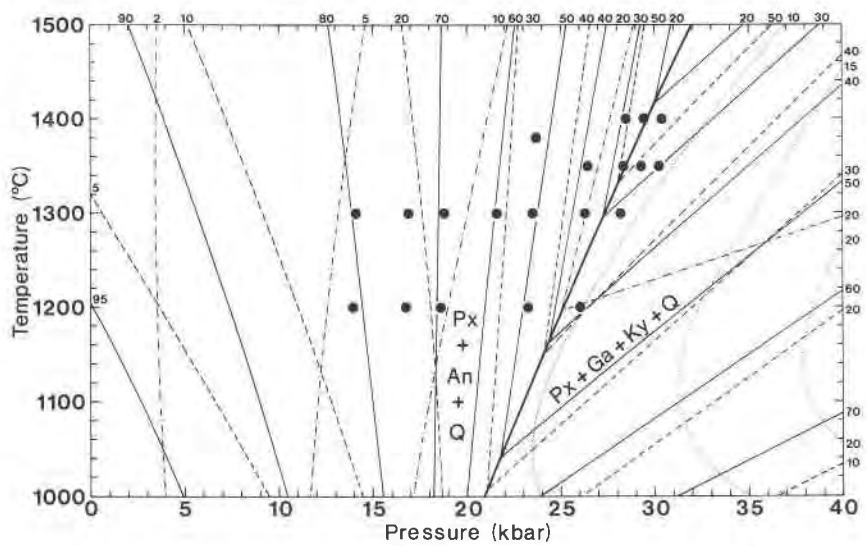

Fig. 2. Subsolidus P-T phase relations in the silica-saturated CMAS system. The heavy line is the univariant curve for Reaction 4. Thin lines are the pyroxene and garnet isopleths in mole percent; solid line = Di; dashed line = CaTs; dash-dot line = CaEs; and dotted line = Py. Solid dots represent the P-T locations of the present experiments with the assemblage Px + An + Q, in some cases metastably in the garnet field. Omitted from the diagram are α-Q = β-Q and Q = Cs transitions.

Table 2. Conditions of equilibration experiments and average compositions of clinopyroxene in equilibrium with phases in the given assemblage and PbO-rich liquid

Run #	T (°C)	P[a] (kb)	t (h.)	Mix[b]	S.[c]	An.[d]	Cations/6 oxygens Ca	Mg	Al	Si	Sum	X_{CaTs}	X_{CaEs}
Assemblage: Px + An + Q													
113	1200	15	8	A	D	32	0.982	0.853	0.253	1.893	3.981	0.108	0.037
118	1300	15	8	B	D	46	0.967	0.865	0.284	1.871	3.987	0.124	0.044
161	1200	18	23	C	D	37	0.968	0.777	0.386	1.838	3.969	0.162	0.063
160	1300	18	26	A	D	27	0.950	0.770	0.430	1.818	3.968	0.176	0.080
117	1200	20	8	C	DC	30	0.961	0.723	0.461	1.812	3.957	0.189	0.083
108	1300	20	8	A	DC	51	0.956	0.699	0.532	1.774	3.961	0.224	0.083
114	1300	23	8	D	D	25	0.934	0.567	0.741	1.694	3.936	0.305	0.130
150	1200	25	8	E	D	14	0.919	0.470	0.894	1.635	3.918	0.365	0.164
102	1300	25	8	D	D	18	0.930	0.490	0.885	1.627	3.932	0.373	0.138
105	1380	25	5	F	DC	53	0.925	0.500	0.881	1.627	3.933	0.368	0.140
120	1200	28	8	G	D	21	0.897	0.380	1.026	1.592	3.895	0.410	0.209
115	1300	28	8	H	DC	27	0.910	0.399	1.005	1.592	3.906	0.411	0.186
112	1350	28	8	I	DC	60	0.915	0.390	1.051	1.559	3.915	0.441	0.169
104	1300	30	8	J	D	7	0.876	0.289	1.198	1.519	3.882	0.475	0.239
97	1350	30	8	K	DC	33	0.884	0.280	1.228	1.497	3.889	0.498	0.225
110	1400	30	5	L	DC	49	0.894	0.300	1.230	1.481	3.905	0.508	0.198
98	1350	31	9	M	D	27	0.869	0.212	1.324	1.466	3.871	0.531	0.258
96	1400	31	5	N	DC	27	0.890	0.243	1.294	1.464	3.891	0.536	0.221
122	1350	32	8	O	DC	49	0.857	0.171	1.376	1.454	3.858	0.545	0.285
82	1400	32	5	N	DC	58	0.869	0.184	1.373	1.444	3.870	0.555	0.261
Assemblage: Px + An													
129	1300	20	8	P	DC	52	0.977	0.570	0.817	1.614	3.978	0.386	0.045
131	1300	20	8	Q	DC	64	0.975	0.474	1.029	1.504	3.982	0.490	0.042
128	1300	20	8	R	DC	53	0.981	0.409	1.166	1.430	3.986	0.563	0.032
130	1300	20	8	S	DC	55	0.979	0.345	1.288	1.372	3.984	0.622	0.036
134	1300	20	8	T	DC	50	0.990	0.210	1.558	1.231	3.989	0.770	0.020
138	1300	20	8	U	DC	44	0.987	0.149	1.670	1.180	3.986	0.823	0.028
133	1300	25	8	R	D	31	0.970	0.352	1.239	1.410	3.971	0.590	0.059
166	1300	27	22	V	D	19	0.951	0.254	1.405	1.344	3.954	0.652	0.095
166	1300	27	22	V	C	25	0.957	0.187	1.552	1.264	3.960	0.731	0.083
175	1400	28	25	W	DC	60	0.951	0.207	1.506	1.292	3.956	0.702	0.093
185	1400	30	24	X	DC	49	0.931	0.175	1.505	1.318	3.929	0.685	0.140
168	1400	31	27	X	DC	31	0.901	0.109	1.590	1.303	3.903	0.696	0.196
147	1400	25	8	Y	C	26	0.989	-	1.971	1.028	3.988	0.975	0.025
165	1450	28	22	Z	C	11	0.973	-	1.932	1.064	3.969	0.943	0.057
92	1440	33	4	$	C	35	0.910	-	1.803	1.193	3.906	0.814	0.186

[a] Nominal pressures; $P_{"real"} = [0.81 + 10^{-4}T(°C)]P_{nominal}$

[b] Bulk compositions of mixes are given in Table 1

[c] Seed crystals from which analyses were obtained: D = diopside, C = Ca-Tschermak pyroxene

[d] The total number of pyroxene analyses accepted from a given experiment

eling (Table 2). Mole fractions of clinopyroxene components were calculated from cations per six oxygens, using the following procedure: $X_{Di} = Mg$, $X_{CaTs} = 2 - Si$, $X_{CaEs\,(1)} = Al - 2X_{CaTs}$, $X_{CaEs\,(2)} = 2(1 - Ca)$, $X_{CaEs} = [X_{CaEs\,(1)} + X_{CaEs\,(2)}]/2 = Al/2 + Si - Ca - 1$. The sum of X_{Di}, X_{CaTs}, and X_{CaEs} was then normalized to one.

The experimental results are summarized in Table 2 and Figures 1 and 2. In most of the experiments, compositional fields obtained from both kinds of seeds partially or completely overlap, suggesting that equilibrium was closely approached and that the calculated average values are good approximations of the equilibrium compositions. All experiments that gave substantially different average compositions from each kind of seed are shown in Figure 1a. In those cases, the equilibrium compositions should be estimated from Figure 1a. In some experiments, it was possible to obtain analyses from the rims of one kind of seed only; hence, the results in those cases represent only a half bracket.

Thermodynamic evaluation of results

Equilibrium in the assemblage Px + An + Q can be described by two reactions:

$$An = CaTs + Q, \quad (1)$$

$$An + 2Q = 2CaEs. \quad (2)$$

Because anorthite and quartz are stoichiometric, the equilibrium conditions corresponding to these reactions may be written as $RT \ln a_{CaTs} + \Delta G_1 = 0$, and $2RT \ln a_{CaEs} + \Delta G_2 = 0$, where $a_{CaTs} = X_{CaTs} \cdot \gamma_{CaTs}$ and $a_{CaEs} = X_{CaEs} \cdot \gamma_{CaEs}$. Equilibrium in the assemblage Px + An can be described by the reaction

$$3An = 2CaTs + 2CaEs. \quad (3)$$

At equilibrium, $2RT \ln(a_{CaTs} \cdot a_{CaEs}) + \Delta G_3 = 0$, where $\Delta G_3 = 2\Delta G_1 + \Delta G_2$. The free-energy change of a reaction was evaluated at a reference temperature of 1573 K, which is in the middle of the temperature range covered by the present experiments: $\Delta G_{T,P} = \Delta H^0_{1573,1} - T\Delta S^0_{1573,1} + [\Delta V^0_{1573,1} - 0.5\Delta(\beta V^0)P]P$. Volume differences for all reactions were calculated using the unit-cell volumes and the coefficients of thermal expansion (α) and compressibility (β) listed by Gasparik (1984a, 1984b). For the CaEs endmember, the unit-cell volume of jadeite, 6.040 J/bar given by Holland (1980), was used as an approximation. This volume is consistent with a linear extrapolation

Table 3. Unit-cell constants of synthetic Di-CaTs clinopyroxenes

Composition (mol %)	a(Å)	b(Å)	c(Å)	β (Deg.)	V (Å^3)	# of obs.
$Di_{100}CaTs_0$	9.7475(12)	8.9232(10)	5.2496(7)	105.853(8)	439.233(124)	30
$Di_{90}CaTs_{10}$	9.7293(10)	8.8976(8)	5.2559(6)	105.969(6)	437.434(109)	38
$Di_{80}CaTs_{20}$	9.7082(8)	8.8647(7)	5.2647(5)	106.063(5)	435.386(86)	38
$Di_{70}CaTs_{30}$	9.6905(8)	8.8341(7)	5.2713(5)	106.127(5)	433.500(88)	34
$Di_{60}CaTs_{40}$	9.6732(8)	8.8033(7)	5.2761(5)	106.161(5)	431.533(91)	35
$Di_{50}CaTs_{50}$	9.6576(9)	8.7716(7)	5.2790(6)	106.188(6)	429.467(100)	32
$Di_{40}CaTs_{60}$	9.6447(8)	8.7392(7)	5.2822(5)	106.166(6)	427.614(92)	31
$Di_{30}CaTs_{70}$	9.6356(9)	8.7216(7)	5.2811(6)	106.164(7)	426.265(103)	31
$Di_{20}CaTs_{80}$	9.6272(9)	8.7000(9)	5.2805(6)	106.149(7)	424.822(101)	30
$Di_{10}CaTs_{90}$	9.6224(8)	8.6801(7)	5.2794(5)	106.111(6)	423.634(91)	33
Di_0CaTs_{100}*	9.6163(8)	8.6575(7)	5.2775(5)	106.088(6)	422.158(88)	32
$(Di_{.20}CaTs_{.80})_{85}CaEs_{15}$	9.5912(12)	8.6943(14)	5.2671(8)	106.321(8)	421.517(146)	24

Note: The uncertainty in the last digit is given in parentheses.
*1 mol% PbO added as flux.

through a single unit-cell volume measurement of pyroxene with the composition containing 15 mol% of CaEs, given in Table 3. McCormick et al. (1984) also suggested that the unit-cell volume of the CaEs endmember is similar to the volume of jadeite, based on the volume measurements of vacancy-containing omphacites from South African kimberlites.

The Di-CaTs binary exhibits a nonideal mixing with respect to volume, as indicated by the unit-cell volume measurements of Newton et al. (1977). Because the CaTs-rich compositions were not sufficiently covered in that study, the measurements were repeated using an automated powder diffractometer system developed by Wechsler (1981) and a CaF_2 standard. Eleven compositions of the Di-CaTs pyroxene were synthesized at 1350°C and 19 kbar for 24 h, and the results of the measurements are given in Table 3 and Figure 3. The calculation of the excess volume did not include sample $Di_{10}CaTs_{90}$ (mol%), because a small amount of grossular (Gr) was present in the synthetic material. Figure 3 shows small discrepancies between the present measurements and the data of Newton et al. (1977) for the Di-rich compositions. However, the present results for the intermediate compositions agree well with the unit-cell volume measurements of Clark et al. (1962).

Mixing properties of the Di-CaTs-CaEs solid solution were obtained by solution modeling of the present data, using the Redlich-Kister equation for a ternary solution (Redlich and Kister, 1948; Gasparik, 1984a). The solution-modeling procedure is similar to the procedure described by Lindsley et al. (1981, p. 165–166). The input phase compositions are manually adjusted within reasonable limits allowed by the data until the residuals are reduced to insignificantly small values. After a number of cycles, a set of parameters is found that satisfies all data. This procedure, however, does not provide a statistical information on the quality of the fit. The results of the modeling follow (units: joules, kelvins, bars):

$$\Delta G_1 = 25\,250 + 14.7T - [1.29 + (20 \times 10^{-7})P]P,$$
$$\Delta G_2 = 32\,010 + 57.0T - [2.48 - (27 \times 10^{-7})P]P,$$

$$\begin{aligned} RT \ln \gamma_C = {} & (10\,000 - 10T - 0.07P)(X_D^2 + X_D X_E) \\ & - (50\,000 - 31.19T + 0.04P) \\ & \cdot(3X_D^2 - 4X_D^3 + 2X_D X_E - 6X_D^2 X_E - 2X_D X_E^2) \\ & - 7000(12X_D^4 - 16X_D^3 + 5X_D^2 \\ & \quad + 3X_D X_E - 20X_D^2 X_E + 15X_D^2 X_E^2 \\ & \quad - 6X_D X_E^2 + 24X_D^3 X_E + 3X_D X_E^3) \\ & - 20\,160(X_E^2 + X_D X_E) \\ & + 14\,760(3X_E^2 - 4X_E^3 + 2X_D X_E - 2X_D^2 X_E \\ & \quad - 6X_D X_E^2) - 5950(-X_D X_E), \end{aligned}$$

$$\begin{aligned} RT \ln \gamma_E = {} & (10\,000 - 10T - 0.07P)(-X_C X_D) \\ & + (50\,000 - 31.19T + 0.04P)(2X_C X_D^2 - 2X_C^2 X_D) \\ & - 7000(6X_C^2 X_D^2 - 3X_C^3 X_D - 3X_C X_D^3) \\ & - 20\,160(X_C^2 + X_C X_D) \\ & + 14\,760(4X_C^3 - 3X_C^2 - 2X_C X_D \\ & \quad + 6X_C^2 X_D + 2X_C X_D^2) \\ & - 5950(X_D^2 + X_C X_D). \end{aligned}$$

$X_{C,D,E}$ are mole fractions of CaTs, Di, and CaEs, respectively, in clinopyroxene.

Discussion

The parameters above were used to calculate the phase relations in the silica-saturated CMAS system shown in Figures 2 and 4. Isopleths, isotherms, and isobars were calculated by simultaneously minimizing the free energy of the corresponding equilibria. This was achieved, for example, at any specified pressure and temperature by varying two compositional variables until the equilibrium conditions for Reactions 1 and 2 were satisfied.

Figure 2 shows two divariant fields representing the stability of the assemblage Px + An + Q at lower pressures and Px + Ga + Ky + Q at higher pressures. The two stability fields are separated by a univariant boundary

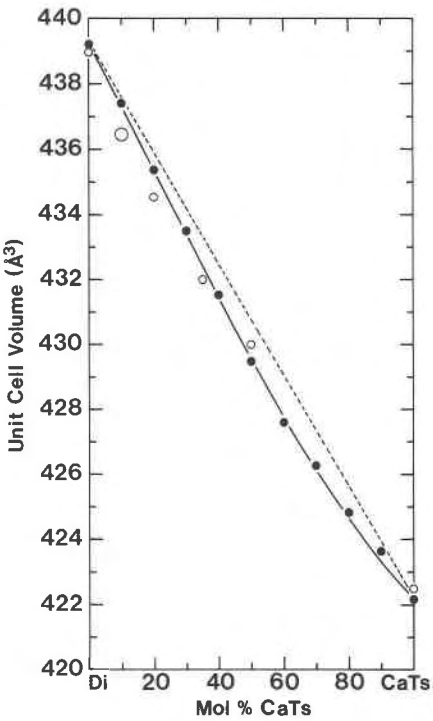

Fig. 3. Unit-cell volume measurements of the Di-CaTs pyroxenes obtained in this study (solid dots) and by Newton et al. (1977) (open circles). The measurements for the $Di_{30}CaTs_{70}$ composition overlap. The size of the symbols is comparable with the uncertainties in the measurements. The solid line is the calculated least-squares fit to the present data; the dashed line indicates ideal mixing.

described by the reaction

$$\text{Px} + \text{An} = \text{Ga} + \text{Ky} + \text{Q}. \quad (4)$$

The reaction was located at pressures only 300 bars lower than the anorthite-breakdown reaction in the CAS system:

$$3\text{An} = \text{Gr} + 2\text{Ky} + \text{Q}. \quad (5)$$

In the stability field of the assemblage Px + An + Q, the pyroxene isopleths intersect at relatively large angles (see Fig. 2); therefore, they are potentially suitable as indicators of both the pressure and the temperature of equilibration. However, the pyroxene composition is mainly pressure dependent, which indicates that the assemblage is a better-geobarometer than geothermometer.

The phase relations of the assemblage Px + Ga + Ky + Q have not been studied experimentally, but can be calculated. Equilibrium in the assemblage is described by the following reactions:

$$3\text{CaTs} + 3\text{Di} = 2\text{Gr} + \text{Py}, \quad (6)$$

$$3\text{CaTs} + 2\text{Q} = \text{Gr} + 2\text{Ky}, \quad (7)$$

$$6\text{CaEs} = \text{Gr} + 2\text{Ky} + 7\text{Q}. \quad (8)$$

The mixing properties of the Gr-Py (pyrope) garnet and the parameters of Reaction 6 were taken from Gasparik (1984a). The free-energy changes of Reactions 7 and 8 can be calculated from ΔG_1, ΔG_2, and the parameters of Reaction 5, for which Gasparik (1984b) gives (units: joules, kelvins, bars): $\Delta G_5 = -42\,100 + 138.0T - (6.31 - (14 \times 10^{-7})P)P$. Thus, for Reactions 7 and 8, $\Delta G_7 = \Delta G_5 - 3\Delta G_1$, and $\Delta G_8 = \Delta G_5 - 3\Delta G_2$. The pyroxene coexisting with Ga + Ky + Q was treated as a ternary Di-CaTs-CaEs solution, although small amounts of En (up to 3 mol%) are also present. Thus, small errors in the position of the calculated isopleths can be expected at higher Py contents owing to this simplification.

In the stability field of the assemblage Px + Ga + Ky + Q, the pyroxene isopleths are significantly more temperature dependent than in the other divariant field (see Fig. 2). The CaEs content changes very slowly with temperature. The garnet composition, however, is mainly pressure dependent. Thus, the best indicators of the equilibrium pressures and temperatures are the combined compositions of the two phases pyroxene and garnet.

The garnet composition is very uniform along the univariant Reaction 4. It varies from $Gr_{92}Py_8$ (mol%) at 1000°C to $Gr_{93}Py_7$ at 1400°C. Similar uniformity of the garnet composition is observed along the spinel lherzolite to garnet lherzolite boundary in the CMAS system, where the experimental evidence indicates a garnet of a constant composition $Gr_{15}Py_{85}$ (Jenkins and Newton, 1979; Perkins and Newton, 1980).

The phase relations in Figure 2 were calculated for the assemblage Px + Ga + Ky + Q containing a Gr-rich garnet. Similar phase relations could be calculated for the same assemblage containing a Py-rich garnet. However, the coexisting pyroxene would contain a significant amount of the En component and would have to be treated as a quaternary solution. The two stability fields of the assemblage Px + Ga + Ky + Q (or coesite, Cs) converge at high pressures in a univariant equilibrium described by the reaction

$$\text{Px} + \text{Ky} = \text{Ga} + \text{Cs}, \quad (9)$$

which is the high-pressure stability limit of the pyroxene in equilibrium with kyanite and coesite. The described phase relations of the assemblage Px + Ga + Ky + Q (or Cs) are very similar to the phase relations of Px + Ga + Cor, the details of which are given by Gasparik (1984a).

Figure 4 shows the calculated phase relations of the assemblage Px + An + Q, projected on the compositional plane Di-CaTs-CaEs as isotherms and isobars. The highest CaEs content in pyroxene at any given temperature is present along the univariant Reaction 4. By calculating the pyroxene compositions along this univariant curve, the maximum solubility limit of the CaEs component in pyroxene in the CMAS system was obtained. The solidus of the assemblage Px + An + Q is not exactly known, but should be near 1400°C. Thus, Figure 4 closely indicates the maximum range of compositions of the pyroxene in equilibrium with anorthite and quartz.

In the CAS system, Gasparik (1984b) calculated the

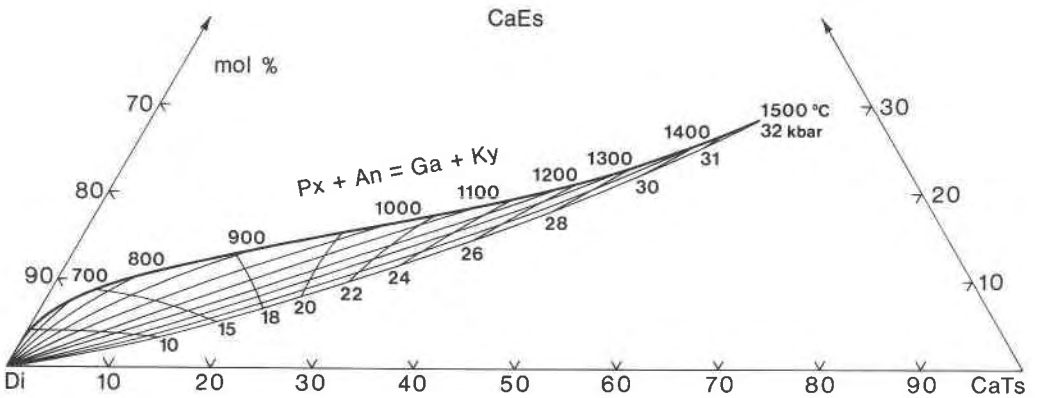

Fig. 4. Phase relations of the assemblage Px + An + Q, with isotherms and isobars (thin lines) projected on the compositional plane Di-CaTs-CaEs. The heavy line is the maximum solubility limit of the CaEs component in pyroxene in the CMAS system, representing pyroxene compositions along the univariant Reaction 4.

location of the univariant reaction

$$\text{An} = \text{Px} + \text{Q} \qquad (10)$$

at 1500°C and 32 kbar. However, Figure 4 indicates almost 12 mol% of the Di component in pyroxene at those conditions. Such a relatively high Di content is directly confirmed by the experiment no. 122, which indicates 17 mol% of Di in pyroxene at the *P-T* conditions essentially corresponding to the univariant Reaction 10, 1350° and 30.2 kbar. At similar conditions (1350°C and 32 kbar nominal), Wood (1979) obtained 24 mol% of Di in the pyroxene coexisting with anorthite and quartz. The observed Di contents, at conditions where Di should not be present, are outside the range of experimental or analytical uncertainties and apparently indicate some anomalous mixing behavior of the Di-CaTs-CaEs pyroxene with the low Di content. Thus, the addition of MgO to the CAS system does not increase the stability of the pyroxene in equilibrium with anorthite and quartz until the Di content of the pyroxene reaches a certain value, e.g., 12 mol% at 1500°C. For this reason, it was not possible to use the parameters for Reaction 1 from the CAS system (Gasparik, 1984b) in the present solution model, which is not capable of reproducing such anomalous behavior. Instead, a different ΔH_1^0 was obtained by solution modeling of the present data, which placed the endmember Reaction 1 at pressures 2.5 kbar higher than indicated by the phase relations in the CAS system. A possible explanation for the inferred deviation from the smooth mixing properties of the ternary pyroxene is ordering, or tendency for the formation of intermediate compounds at various ternary compositions, which is highly probable in the vacancy-containing pyroxenes.

Acknowledgments

This study was conducted under careful guidance of D. H. Lindsley, for which I am very grateful. I also thank J. E. Grover, C. T. Herzberg, R. O. Sack, and B. J. Wood, who provided helpful comments to various earlier drafts of this manuscript, and R. C. Newton, D. Perkins, and G. Sen for the review of the final manuscript. The research was supported by NSF Grants EAR 80-25260 to D. H. Lindsley and EAR 81-07110 to R. C. Newton.

References

Bence, A.E., and Albee, A.L. (1968) Empirical correction factors for the electron microanalysis of silicates and oxides. Journal of Geology, 76, 382–403.

Clark, S.P., Jr., Schairer, J.F., and de Neufville, J. (1962) Phase relations in the system $CaMgSi_2O_6$-$CaAl_2SiO_6$-SiO_2 at low and high pressure. Carnegie Institution of Washington Year Book 61, 59–68.

Gasparik, T. (1981) Thermodynamic properties of pyroxenes in the NCMAS system saturated with silica. Ph.D. Thesis, State University of New York at Stony Brook.

——— (1984a) Experimentally determined stability of clinopyroxene + garnet + corundum in the system CaO-MgO-Al_2O_3-SiO_2. American Mineralogist, 69, 1025–1035.

——— (1984b) Experimental study of subsolidus phase relations and mixing properties of pyroxene in the system CaO-Al_2O_3-SiO_2. Geochimica et Cosmochimica Acta, 48, 2537–2545.

——— (1985) Experimental study of subsolidus phase relations and mixing properties of pyroxene and plagioclase in the system Na_2O-CaO-Al_2O_3-SiO_2. Contributions to Mineralogy and Petrology, 89, 346–357.

Gasparik, T., and Lindsley, D.H. (1980) Phase equilibria at high pressure of pyroxenes containing monovalent and trivalent ions. In C.T. Prewitt, Ed. Pyroxenes, 309–339. Mineralogical Society of America Reviews in Mineralogy, 7.

Holland, T.J.B. (1980) The reaction albite = jadeite + quartz determined experimentally in the range 600–1200°C. American Mineralogist, 65, 129–134.

Jenkins, D.M., and Newton, R.C. (1979) Experimental determination of the spinel peridotite to garnet peridotite inversion at 900°C and 1,000°C in the system CaO-MgO-Al_2O_3-SiO_2, and at 900°C with natural garnet and olivine. Contributions to Mineralogy and Petrology, 68, 407–419.

Lindsley, D.H., Grover, J.E., and Davidson, P. M. (1981) The thermodynamics of the $Mg_2Si_2O_6$-$CaMgSi_2O_6$ join: A review and an improved model. In R.C. Newton, A. Navrotsky, and B.J. Wood, Eds. Thermodynamics of minerals and melts, 149–175. Advances in physical geochemistry, 1, Springer-Verlag, New York.

McCormick, T.C., Smyth, J.R., and Buseck, P.R. (1984) Crystal chemistry of vacancy-bearing mantle omphacites. EOS (American Geophysical Union Transactions), 65, 306.

Newton, R.C., Charlu, T.V., and Kleppa, O.J. (1977) Thermochemistry of high pressure garnets and clinopyroxenes in the

system CaO-MgO-Al_2O_3-SiO_2. Geochimica et Cosmochimica Acta, 41, 369–377.

Perkins, D., and Newton, R.C. (1980) The compositions of coexisting pyroxenes and garnet in the system CaO-MgO-Al_2O_3-SiO_2 at 900°–1,100°C and high pressures. Contributions to Mineralogy and Petrology, 75, 291–300.

Redlich, O., and Kister, A.T. (1948) Thermodynamics of nonelectrolyte solutions. Algebraic representation of thermodynamic properties and the classification of solutions. Industrial and Engineering Chemistry, 40, 345–348.

Wechsler, B.A. (1981) Crystallographic studies of titanomagnetites and ilmenite. Ph.D. Thesis, State University of New York at Stony Brook.

Wood, B.J. (1979) Activity-composition relationships in $Ca(Mg,Fe)Si_2O_6$-$CaAl_2SiO_6$ clinopyroxene solid solutions. American Journal of Science, 279, 854–875.

Wood, B.J., and Henderson, C.M.B. (1978) Compositions and unit-cell parameters of synthetic nonstoichiometric tschermakitic clinopyroxenes. American Mineralogist, 63, 66–72.

Manuscript received June 18, 1984
Manuscript accepted January 14, 1986